Materials Research Bulletin 46 (2011) 2199–2203

Contents lists available at SciVerse ScienceDirect

Materials Research Bulletin

journal homepage: www.elsevier.com/locate/matresbu

Vapor-phase synthesis of a solid precursor for α-alumina through a catalytic decomposition of aluminum triisopropoxide

Tu Quang Nguyen [a], Kyun Young Park [a,*], Kyeong Youl Jung [a], Sung Baek Cho [b]

[a] Department of Chemical Engineering, Kongju National University, 275 Budae-dong, Cheonan, Chungnam 330-717, Republic of Korea
[b] Korea Institute of Geoscience & Mineral Resources (KIGAM), 92 Gwahang-no, Yuseong-gu 305-350, Republic of Korea

ARTICLE INFO

Article history:
Received 12 October 2010
Received in revised form 13 May 2011
Accepted 14 September 2011
Available online 21 September 2011

Keywords:
A. Ceramics
B. Chemical synthesis
C. Thermogravimetric analysis
C. X-ray diffraction

ABSTRACT

A new solid precursor, hydrous aluminum oxide, for α-alumina nanoparticles was prepared by thermal decomposition of aluminum triisopropoxide (ATI) vapor in a 500 mL batch reactor at 170–250 °C with HCl as catalyst. The conversion of ATI increased with increasing temperature and catalyst content; it was nearly complete at 250 °C with the catalyst at 10 mol% of the ATI. The obtained precursor particles were amorphous, spherical and loosely agglomerated. The primary particle size is in the range 50–150 nm. The ignition loss of the precursor was 24%, considerably lower than 35% of $Al(OH)_3$, the popular precursor for alumina particles. Upon calcination of the precursor at 1200 °C in the air with a heating rate of 10 °C/min and a holding time of 2 h, the phase was completely transformed into α. The spherical particles composing the precursor turned worm-like by the calcination probably due to sintering between neighboring particles. The surface area equivalent diameter of the resulting α-alumina was 75 nm.

1. Introduction

α-Alumina is one of the most important oxides because of its high melting point, high wear resistance, high electrical insulation, good chemical, thermal, and mechanical stability [1]. The unique properties of α-alumina make it useful in a variety of applications including catalyst, polishing, electronic, and bioceramics [2,3].

Increasing attention has been paid to the development of nano-sized α-alumina particles. Park et al. [2] reported a preparation of 50 nm α-alumina by sol–gel processing of aluminum triisopropoxide (ATI). A solution method of producing 100 nm α-alumina particles using a seed crystal has been patented [4]. Recently, nanosized γ-alumina particles were produced by neutralization of aluminum chloride solution with bases at ambient temperature [5,6] or by thermal decomposition of a mixture of sucrose and aluminum nitrate solution at 400 °C [7]. The calcination of the γ-alumina particles derived from the thermal decomposition led to α-alumina particles, 44–55 nm in size. In contrast to these liquid-phase methods that involve a series of time consuming steps such as filtration, washing and drying, vapor-phase methods capable of producing dry nanoparticles in one step were reported by which trimethylaluminum (TMA), aluminum tri-*sec*-butoxide (ATBO), or anhydrous aluminum chloride vapor was oxidized, decomposed, or hydrolyzed [8–10].

ATI is less hazardous than TMA and higher in aluminum content than ATBO. ATI has been used for vapor-phase preparation of thin films [11,12]. To our knowledge, however, there is no report on the vapor-phase preparation of particles using ATI. The admission of ATI vapor into a flame would probably yield alumina nanoparticles similar in structure to the fumed alumina that has been commercially produced by flame hydrolysis of aluminum chloride vapor. The alumina particles produced from the flame process are known to be severely agglomerated due to the high temperature, and the phase of which is a mixture of γ, δ, and α. To obtain α-alumina particles based on any vapor-phase method, two stages may be required; in the first stage amorphous or transient alumina particles are produced and in the second stage these particles are calcined for hours to transform the phase into α.

In the present study, solid particles that can be used as precursor for nano-sized α alumina were prepared by decomposition of ATI vapor at a temperature of about 200 °C. The use of such a low temperature is an advantage, compared with the high-temperature flame process. ATI, which is solid at ambient condition, was vaporized and decomposed with HCl as catalyst. The particles as-produced are not alumina but intermediates, $AlO_xCl_y(OH)_z$, which turned into α-alumina upon calcination. The conversion of ATI and the particle size and morphology of the alumina precursor were investigated under varying decomposition conditions. The calcination condition for the transformation into α-alumina was studied.

* Corresponding author. Tel.: +82 41 521 9354; fax: +82 41 554 2640.
E-mail address: kypark@kongju.ac.kr (K.Y. Park).

0025-5408/$ – see front matter © 2011 Elsevier Ltd. All rights reserved.
doi:10.1016/j.materresbull.2011.09.011

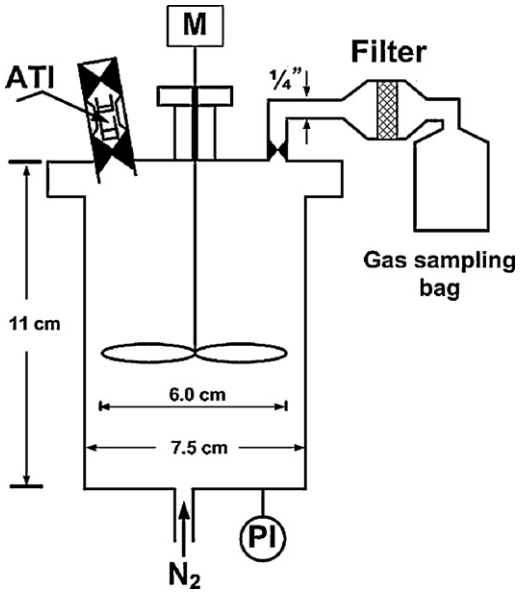

Fig. 1. Schematic drawing of experimental setup.

2. Experimental

2.1. Experimental procedure

The experimental setup is schematically shown in Fig. 1. A 500 mL batch reactor was used for the decomposition. The reactor is equipped with an electrically driven stirrer, a thermocouple, a pressure gauge, a precursor feeder, a filter at the reactor outlet and a gas sampling bag after the filter. The ATI feeder is a stainless steel pipe, 0.8 cm in inside diameter and 5 cm in length, with two valves at both ends. The detailed description of the apparatus is available elsewhere [10].

0.03 g of ATI (Aldrich, 98%) and 1.3 μL of 36 wt.% HCl (Samchun Pure Chem. Co. LTD) were loaded in two cylindrical glass boats, respectively. These boats were then put in the feeder. The feeder containing the two boats was mounted vertically on the top of the reactor. By opening the lower valve of the feeder, the ATI-laden boat was dropped by gravity to the reactor set at a predetermined temperature under nitrogen atmosphere. The evaporation of the ATI was confirmed with the pressure rise. Following the ATI evaporation, the HCl-laden boat was dropped to the reactor for HCl evaporation. Following the two-stage evaporation, the decomposition reaction was continued for a given residence time. Upon termination of a reaction, the product gas was sampled by the gas sampling bag and analyzed with a gas chromatography analyzer. The produced particles were carried out of the reactor by a flow of nitrogen supplied from the bottom, and collected in the filter. The as-produced particles were calcined in a box furnace for transformation into α-phase alumina.

2.2. Characterization

The morphology of the particles was examined by scanning electron microscopy (SEM) (JEOL, JSM-6700), the crystalline structure by X-ray diffraction with Cu-Kα radiation (Rigaku, D/MAX-RB) and the molecular structure by FT-IR spectroscopy (Perkin Elmer, Spectrum GX). The chemical composition of the particles was determined by energy dispersive X-ray analysis (EDX) and X-ray photoelectron spectroscopy (XPS) (ESCA 2000). The surface area of the particles was measured by nitrogen adsorption using a Micromeritics ASAP 2010 instrument. The mass loss of the particles upon heating in an alumina boat was measured with a thermogravimetric analyzer (TA Instruments, SDT2960). The number-average particle diameter was determined with an image analyzer (Media Cybernetics, Image-Pro plus 40) through diameter measurement of about 300 particles. The propylene content in the product gas was determined by gas chromatography (Hewlett Packard, Model HP5890) with a packaged column (Chromosorb 102) and a flame ionization detector. The conversion of ATI was then calculated from the propylene content using the stoichiometry of the reaction [13]:

$$Al(OC_3H_7)_3 \rightarrow 0.5Al_2O_3 + 3C_3H_6 + 1.5H_2O.$$

3. Results and discussion

3.1. Effect of catalyst content

The molar ratio of catalyst to ATI was varied from 0 to 0.1, holding the temperature at 200 °C and the reaction residence time at 30 min. Three runs were made for each condition. Fig. 2 shows the conversions of ATI at different HCl/Al molar ratios. The conversion was 38.1% in the absence of catalyst. The conversion increased to 70.0% at the ratio of 0.01, and to 83.7% as the ratio was further increased to 1.0. This may be the first discovery that HCl is effective in catalyzing the vapor-phase decomposition of ATI, although HCl has been used as catalyst in sol–gel preparation of metal oxide particles [14].

There is a report that a proton transfer could occur in the presence of water vapor for a gas-phase HCl–NH_3 reaction system [15]. Assuming that the gas-phase proton transfer is possible in the present system because water vapor is available from the vaporization of the aqueous HCl provided as a source for the catalyst, the role of HCl in the decomposition of ATI, a weak base, is proposed as follows:

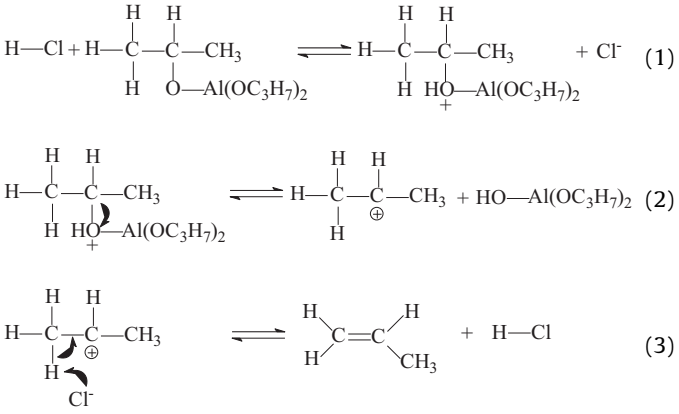

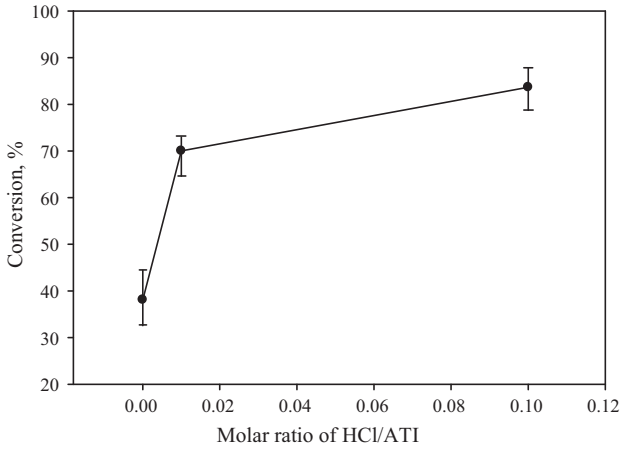

Fig. 2. Effect of HCl/ATI molar ratio on the conversion of ATI.

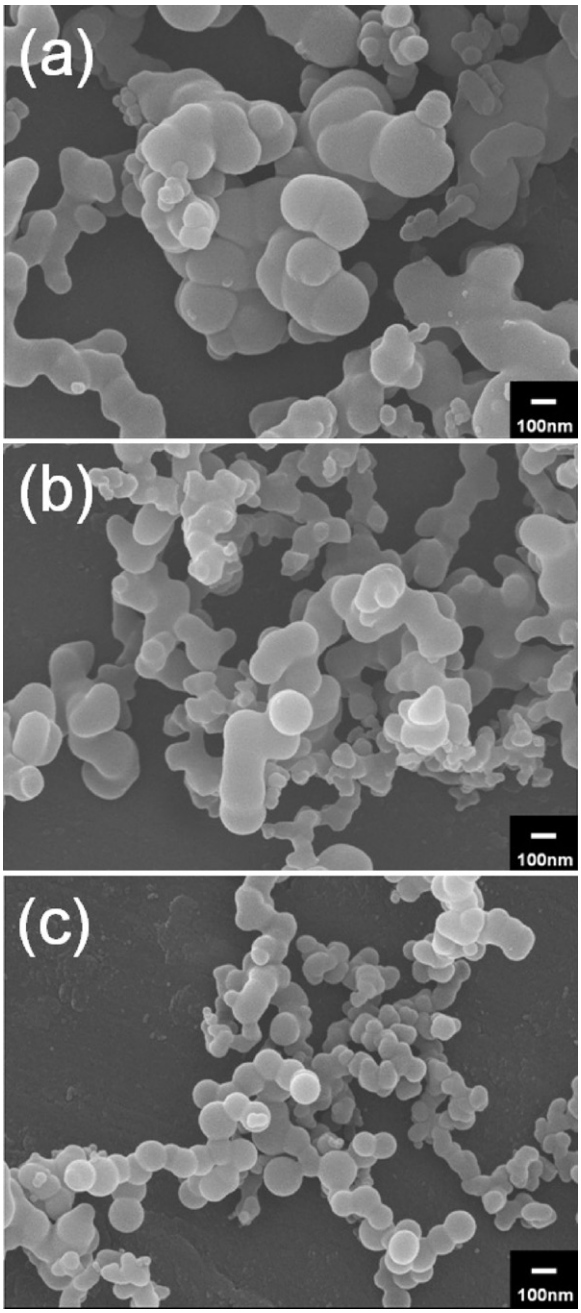

Fig. 3. Scanning electron microscopic images of particles produced at various HCl/ATI molar ratios (a) 0, (b) 0.01, and (c) 0.1 (reaction time: 30 min, reaction temperature: 200 °C).

The catalyzing acid gives the protonated alkoxide and the conjugate base of the acid in Eq. (1). In Eq. (2), the protonated alkoxide undergoes heterolysis to form the carbocation and hydride. Finally, in Eq. (3), the carbocation loses a proton to the base to yield propylene. A condensation polymerization follows between resulting hydroxide molecules to form a dimer.

$$(C_3H_7O)_2Al(OH) + [(OH)Al(OC_3H_7)_2] \rightarrow [(C_3H_7O)_2Al{-}O{-}Al(OC_3H_7)_2] + H_2O. \quad (4)$$

By successive hydride formation in Eq. (2) and condensation polymerization, the dimeric species in Eq. (4) continues to grow with its vapor pressure decreasing, and eventually leads to a particle. The proposed mechanism requires verification in the future.

Fig. 3 shows the scanning electron microscopic images of the alumina precursor particles obtained at various HCl/ATI molar ratios. The particle size decreased, but the sphericity increased with increasing the ratio from 0 to 0.01 and 0.1. An increase in the ratio increased the decomposition rate, as shown in Fig. 2, and successively increased the nucleation rate to have resulted in smaller primary particles.

3.2. Effect of decomposition temperature

The reactor temperature was varied from 170 to 250 °C, holding the residence time at 30 min and the HCl/ATI ratio at 0.1. Fig. 4 shows the effect of decomposition temperature on the conversion of ATI. The conversion was 62.4% at 170 °C and increased to 96.0% at 250 °C.

The particles obtained at 170 °C were agglomerated and irregular in shape. It was difficult to identify particle boundaries. By comparison, the particles obtained at higher temperatures were less agglomerated, spherical, and narrower in size distribution. The number-average particle diameter decreased with increasing temperature: 105, 94 and 81 nm at 200, 230 and 250 °C, respectively. In the gas-phase synthesis of titania particles, some investigators [16,17] reported a similar decrease in particle diameter with increasing temperature, while other studies [18,19] showed an increase. An increase in temperature would increase the collision-coalescence rate and the nucleation rate. The collision-coalescence contributes to particle growth, while the nucleation increases the number of particles and consequently acts to make primary particles smaller. At the temperature level of the present study, the nucleation rate appears to be the dominant factor to yield the observed temperature dependency.

Fig. 5 shows the effect of decomposition temperature on the chlorine content in the particles. The chlorine content was 3.0 at.% at 170 °C and decreased to 1.2 at.% at 250 °C. The source of chlorine must be the HCl added as catalyst. The catalyst participated in the reaction appears not to have been recovered completely.

3.3. Thermogravimetric analysis of as-produced particles

The particles produced at the decomposition temperature of 200 °C with the residence time at 30 min and the molar ratio of HCl/ATI at 0.1 were heated in oxygen atmosphere up to 1200 °C at a heating rate of 10 °C/min. As shown in Fig. 6, the mass decreased with temperature increase due to the removal of volatiles. The mass was 69% of the initial value at 1080 °C. Thereafter, the mass rather increased to 76% at 1200 °C and leveled off. Such an extraordinary increase in mass was absent with $Al(OH)_3$, a

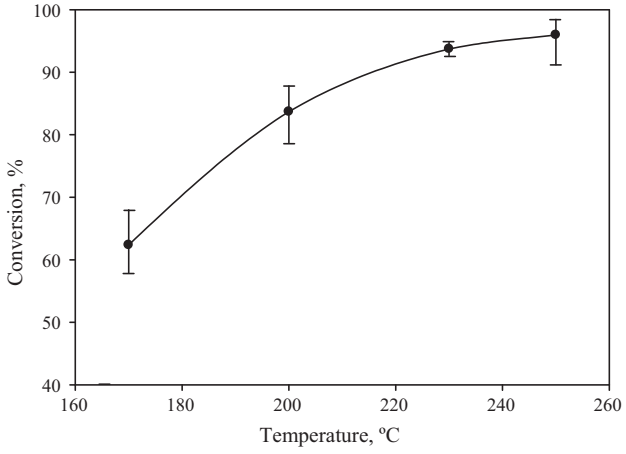

Fig. 4. Effect of temperature on conversion of ATI.

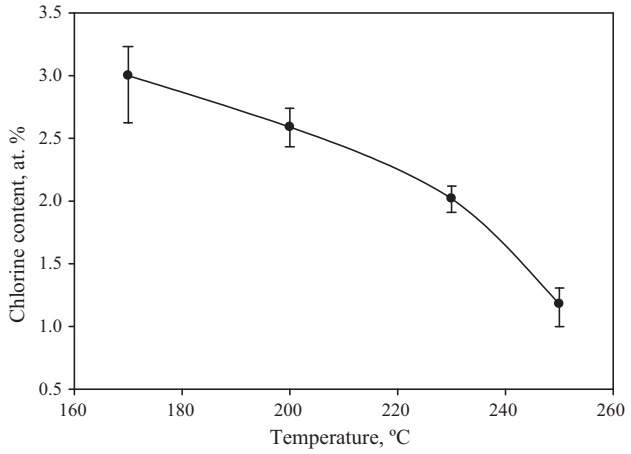

Fig. 5. Effect of temperature on chlorine content of as-produced particles.

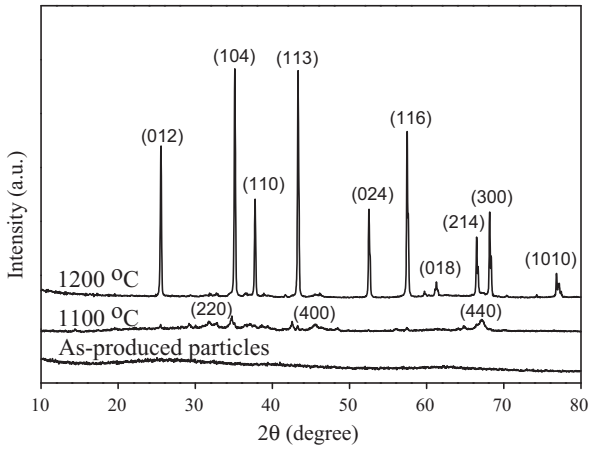

Fig. 7. XRD patterns of as-produced particles at different calcination temperatures.

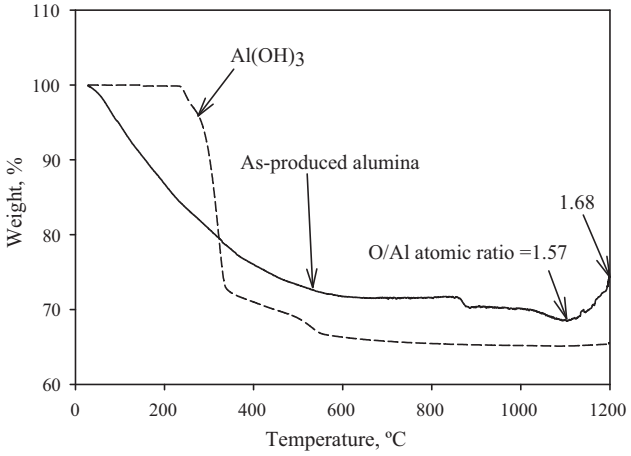

Fig. 6. Thermogravimetric analysis of as-produced particles.

conventional precursor for alumina. The ignition loss of the present alumina precursor amounts to 24%, considerably lower than that of $Al(OH)_3$.

By XPS analysis, the atomic ratio of oxygen to aluminum was 1.57 at 1080 °C and 1.68 at 1200 °C. The stoichiometric atomic ratio of Al_2O_3 is 1.5. The increase in the ratio by increasing the temperature from 1080 to 1200 °C was consistent. This supports that the mass increased due to oxygen. A formation of aluminum peroxide, which should give an atomic ratio higher than 1.5, was reported for the reaction of α-alumina with platinum [20]. In the present study, however, no source of platinum was present. An existence of oxygen vacancies was reported for alumina films in contact with NiAl [21]. Any oxygen vacancy in the aluminum oxide particles at 1080 °C may be filled with ambient oxygen to increase the mass. But, it is questionable that the aluminum sub-oxide can exist under the operating condition. Further studies may be necessary to investigate the causes of the mass increase.

3.4. Calcination of as-produced particles for α-alumina

The particles produced at the decomposition temperature of 200 °C with the residence time at 30 min and the molar ratio of HCl/ATI at 0.1 were calcined for 2 h at 1100 and 1200 °C. Fig. 7 shows a comparison in XRD pattern between as-produced and calcined particles. The as-produced particles are amorphous. At 1100 °C, peaks indicative of γ-alumina [JCPDS 81-2267] appeared. At 1200 °C, all the peaks are assigned to α-alumina phase [JCPDS 10-0425]. The approximate crystallite size of the α-alumina was determined to be 47 nm, using Scherrer's equation:

$$D = \frac{0.9\lambda}{\beta \cos\theta},$$

where D is the crystallite size, λ is the wave length of the X-ray, and β is the full width at half the maximum intensity. The broadening due to the machine was neglected.

FT-IR spectra of as-produced and calcined particles are shown in Fig. 8. In the spectra of the as-produced particles, two peaks indicating the presence of $\nu CH(-CH_3)$ and $\nu CH(-CH_2-)$ groups were observed at 2920 and 2850 cm^{-1}, respectively [22]. Those peaks disappeared in the calcined particles. The peak at 1630 cm^{-1} due to the OH bonding vibration mode [23] decreased in strength after calcination. A sharp peak at 562 cm^{-1} representing α-alumina [24] appeared in the spectra of the calcined particles.

Fig. 9 shows the scanning electron microscopic images of the alumina particles obtained by calcination at 1100 and 1200 °C, respectively. The morphology of the as-produced particles was maintained at 1100 °C. The particle size, however, decreased probably due to the removal of volatiles and densification. As the calcination temperature was increased further to 1200 °C, the particles turned worm-like due to sintering between neighboring particles. The BET surface area was measured to be 20 m^2/g. The surface-area equivalent diameter was calculated to be 75 nm using the alumina density of 3.98 g/cm^3. By EDX analysis, the calcined particles are free of residual chlorine.

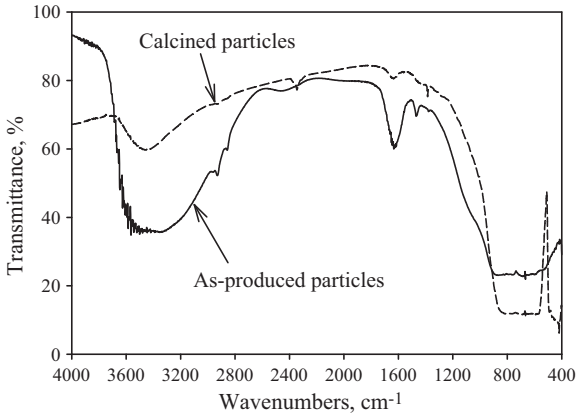

Fig. 8. FT-IR spectra of as-produced particles and calcined particles.

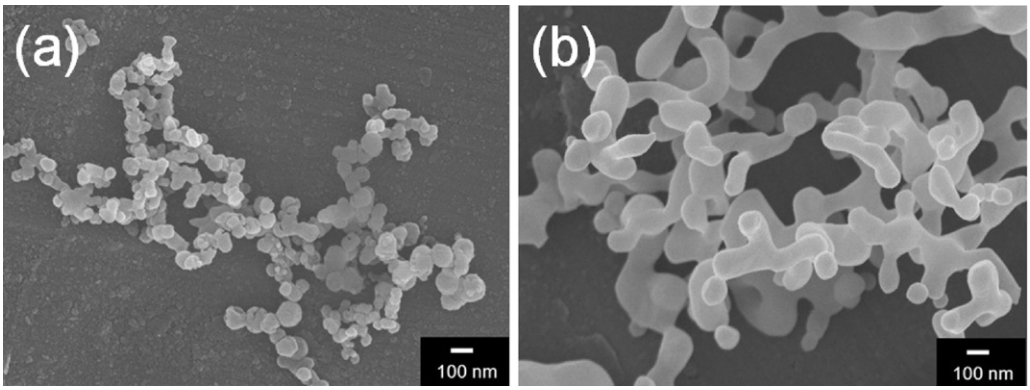

Fig. 9. Scanning electron microscopic images of obtained particles after calcination at (a) 1100 °C and (b) 1200 °C.

4. Conclusion

A solid particulate precursor for α-alumina was prepared through a thermal decomposition of ATI vapor at 170–250 °C with HCl as a catalyst. The decomposition was nearly complete at 250 °C with the molar ratio of HCl to ATI at 0.1. α-Alumina particles, 75 nm in surface area equivalent diameter, were obtained by calcining the precursor at 1200 °C for 2 h. The ignition loss of the precursor was 24%, considerably lower than that of $Al(OH)_3$, a conventional alumina precursor. The obtained α-alumina exhibited a worm-like structure due to sintering between neighboring particles. The unique structure of these α-alumina particles may suggest their application as raw materials for ceramic filters, catalyst supports for high temperature reactions, reinforcing fillers for polymers, and fine abrasives.

Acknowledgement

This research was supported by a grant from the Fundamental R&D Program for Core Technology of Materials funded by the Ministry of Knowledge Economy, Republic of Korea.

References

[1] R.J. Yang, F.S. Yen, S.M. Lin, C.C. Chen, J. Cryst. Growth 299 (2007) 429–435.
[2] Y.K. Park, E.H. Tadd, M. Zubris, R. Tannenbaum, Mater. Res. Bull. 40 (2005) 1506–1512.
[3] A.I.Y. Tok, F.Y.C. Boey, X.L. Zhao, J. Mater. Process. Technol. 178 (2006) 270–273.
[4] H. Maki, Y. Takeuchi, US Patent 7,351,394 B2 (2008).
[5] A. Majhi, G. Pugazhenthi, A. Shukla, Ind. Eng. Chem. Res. 49 (2010) 4710–4719.
[6] Y. Mathieu, L. Vidal, V. Valtchev, B. Lebeau, New J. Chem. 33 (2009) 2255–2260.
[7] C.H. Lim, S. Santra, S. Sahu, A. Aziz, P. Pramanik, Int. J. Nanotechnol. 7 (2010) 1003–1012.
[8] E. Borsella, S. Botti, R. Giorgi, S. Martelli, S. Turtu, G. Zappa, Appl. Phys. Lett. 63 (1993) 1345–1347.
[9] P. Moravec, J. Smolik, V.V. Levdansky, J. Mater. Sci. Lett. 20 (2001) 311–313.
[10] Y.S. Yoo, K.Y. Park, K.Y. Jung, S.B. Cho, Mater. Lett. 63 (2009) 1844–1846.
[11] D.C. Cameron, L.D. Irving, G.R. Jones, J. Woodward, Thin Solid Films 91 (1982) 339–348.
[12] A.N. Gleizes, C. Vahlas, M.M. Sovar, D. Samelor, M.C. Lafont, Chem. Vap. Deposition 13 (2007) 23–29.
[13] O. Mekasuwandumrong, P.L. Silveston, P. Praserthdam, M. Inoue, V. Pavarajarn, V. Tanakulrungsank, Inorg. Chem. Commun. 6 (2003) 930–934.
[14] C.J. Brinker, G.W. Scherer, Sol–Gel Science: The Physics and Chemistry of Sol–Gel Processing, Academic Press, New York, 1990.
[15] J.A. Snyder, R.A. Cazar, A.J. Jamka, F.M. Tao, J. Phys. Chem. A 103 (1999) 7719–7724.
[16] Y. Suyama, A. Kato, J. Am. Ceram. Soc. 59 (1976) 146–149.
[17] H.D.H.D. Jang, J. Jeong, Aerosol Sci. Technol. 23 (1995) 553–560.
[18] M. Formenti, F. Juillet, P. Meriaudeau, S.J. Teichner, P. Vergnon, in: G.M. Hidy (Ed.), Aerosols and Atmospheric Chemistry, Academic Press, New York, 1972.
[19] M.K. Akhtar, Y. Xiong, S.E. Pratsinis, AIChE J. 37 (1991) 1561–1570.
[20] Y.C. Lu, R.R. Dieckmann, S.L. Sass, Acta Metall. Mater. 42 (1994) 1125–1137.
[21] M. Schmid, M. Shishkin, G. Kresse, E. Napetschnig, P. Varga, M. Kulawik, N. Nilius, H.P. Rust, H.J. Freund, Phys. Rev. Lett. 97 (2006) 046101.
[22] K.M.S. Khalil, Appl. Surf. Sci. 255 (2008) 2874–2878.
[23] J. Chandradass, M. Balasubramanian, Ceram. Int. 31 (2005) (2005) 743–748.
[24] S. Wang, X. Li, S. Wang, Y. Li, Y. Zhai, Mater. Lett. 62 (2008) 3552–3554.